A Shear-compression Specimen for Large Strain Testing

by D. Rittel, S. Lee and G. Ravichandran

ABSTRACT—A new specimen geometry, the shear-compression specimen (SCS), has been developed for large strain testing of materials. The specimen consists of a cylinder in which two diametrically opposed slots are machined at 45° with respect to the longitudinal axis, thus forming the test gage section. The specimen was analyzed numerically for two representative material models, and various gage geometries. This study shows that the stress (strain) state in the gage, is three-dimensional rather than simple shear as would be commonly assumed. Yet, the dominant deformation mode in the gage section is shear, and the stresses and strains are rather uniform. Simple relations were developed and assessed to relate the equivalent true stress and equivalent true plastic strain to the applied loads and displacements. The specimen was further validated through experiments carried out on OFHC copper, by comparing results obtained with the SCS to those obtained with compression cylinders. The SCS allows to investigate a large range of strain rates, from the quasi-static regime, through intermediate strain rates (1–100 s^{-1}), up to very high strain rates (2×10^4 s^{-1} in the present case).

KEY WORDS—Shear, large strain, testing, shear-compression specimen

Introduction

Large shear strains are found in many applications, such as (high-speed) machining, ballistic failure, ductile fracture, and micromechanics of void growth and coalescence. The large strain constitutive behavior of a material has therefore to be determined for modeling and calculation purposes.[1] Contrary to uniaxial tensile testing, shear testing is complicated by the fact that a state of pure (or even simple) shear is not easily achievable in most specimen geometries. While a review of the available specimen geometries is beyond the scope of this paper, it can be noted that a wide body of research has been dedicated to high-strain-rate applications. For example, thin walled torsion specimens have been used in a Kolsky (split Hopkinson) torsion bar apparatus.[2] Large shear strains can also be achieved by devising a suitable specimen geometry that transforms the linear displacement into local shear. An early shear-tensile specimen was developed by Hundy and Green.[3] Another example of such a specimen is the so-called "hat specimen" which was developed by Meyer and Manwaring,[4] and used thereafter by many other researchers. Another variant is the double shear specimen used by Klepaczko.[5] Finally, at very high strain rates, a very simple specimen geometry (thin foil) has been used by Clifton and Klopp[6] in their pressure-shear plate impact experiments. For all the specimens used in high-strain-rate testing, a common issue of concern is that of the nature and uniformity of the strain (stress) field in the gage section of the specimen. While this issue has to be examined by numerical techniques, uniformity is currently assumed so that simple relations can be used to determine the nominal strain and stress in the specimen. Such relations, which are deemed to represent the average strain and stress state in the shear region, are derived from the specimen geometry and prescribed displacements or loads. Consequently, one would like to have a "simple" and well characterized specimen which can be used to investigate the large strain material response over a wide range of strain rates.

The purpose of this work is to report a new and relatively simple framework which has been developed to allow for large (shear dominated) strain testing of materials. The paper is organized in two main parts. The first addresses the new specimen (SCS, shear-compression specimen) and its characterization. The SCS is described and the relevant load and displacement parameters are outlined. Results of the stress analysis are shown and discussed here. In the following section, the approximate formulas to be used for the determination of the equivalent stress, strain and strain rate are presented and discussed. The second part of the paper addresses the experimental validation of the SCS. Experimental results on the high-strain-rate response of oxygen free (OFHC) copper are shown and discussed. Typically, we compare the equivalent stress–strain data obtained with the shear specimen to those obtained from uniaxial compression of cylindrical specimens (CS). Very good agreement is noted in a similar range of strain rates (typically up to 9000 s^{-1}) between the results for the two types of specimens (SCS and CS). Additional data are shown for higher strain rates achieved with the SCS (typically up to 18000 s^{-1}), beyond the range of achievable strain rates in uniaxial compression. The main results of this work are then discussed and summarized in the concluding sections.

The Specimen and Its Analysis

The Shear Compression Specimen (SCS)

The shear compression specimen is schematically depicted in Fig. 1. The SCS is very simple: it consists of a short cylinder into which two slots have been machined

D. Rittel (SEM Member) is a Visiting Professor, S. Lee is a Postdoctoral Associate, and G. Ravichandran is a SEM Member, Graduate Aeronautical Laboratories, California Institute of Technology, Pasadena, CA 91125, USA. D. Rittel is on sabbatical leave from Technion, Israel Institute of Technology, Faculty of Mechanical Engineering, 32000 Haifa, Israel.

Original manuscript submitted: August 17, 2000.
Final manuscript received: September 24, 2001.

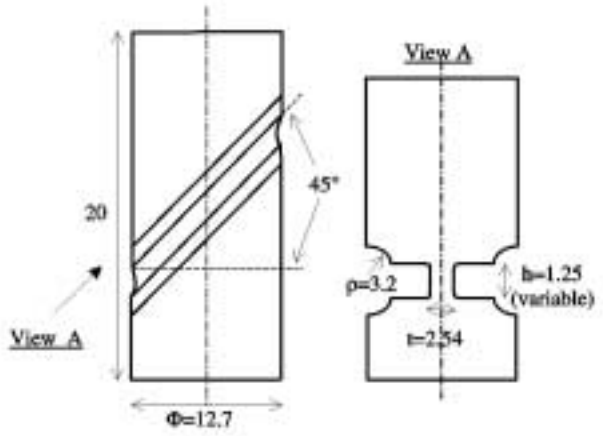

Fig. 1—Schematic representation of the shear compression specimen. All dimensions are in mm. h, t and ϕ are the geometrical parameters used for stress and strain determination.

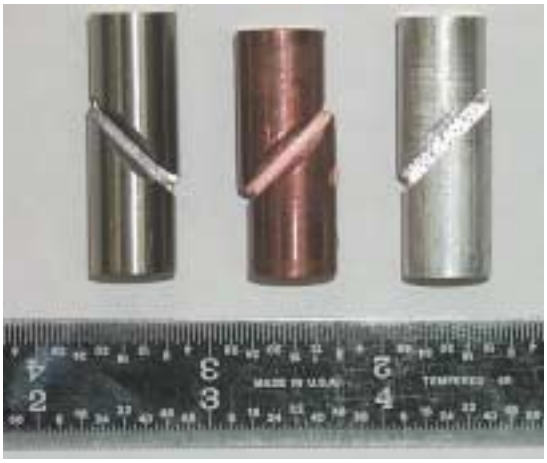

Fig. 2—Photographs of deformed specimens. From left to right: annealed Ti-6Al-4V titanium alloy, commercial OFHC copper and 6061-T351 aluminum alloy. The shear dominated deformation of the gage section is noticeable.

at 45° to the longitudinal axis. The key idea is that upon longitudinal compression of the cylinder, the gage section will be subjected to a dominant state of shear deformation. The deforming gage is defined by its height (h) and thickness (t). The diameter of the cylindrical sections (Φ) is chosen such that they remain elastic during the test. These sections prescribe and transfer the vertical displacements and loads to the gage section. A clearance (ρ) is machined in the specimen, to provide visual access to the gage and facilitate diagnostics (e.g. real-time temperature monitoring, or deformation related features). The clearance does not affect load transmission to the gage section. Typical deformed metallic specimens are shown in Fig. 2. In this figure the shear dominated nature of the gage deformation is clearly illustrated.

Numerical Analysis of the Shear Compression Specimen

Computational Model

The stress and strain states of the specimen were determined numerically using finite element analysis. This stage of the specimen development is needed to firmly establish certain assumptions and to extract simple relationships for the equivalent stress and strain. The numerical model is also needed to address specific important issues, such as:

- boundary conditions for the gage section, i.e. how is the prescribed global displacement transferred to the deforming gage section;
- nature of the stress and strain field, i.e. three-dimensional nature of the fields and dominance of specific component;
- uniformity of these fields, to establish assumptions of stress (strain) homogeneity;
- influence of the cylindrical sections of the specimen, to verify that these sections just transfer loads and displacements without permanent deformation;
- influence of the constitutive law, to verify that the results obtained are independent of the nature of the investigated materials. Such response is expected when the boundary conditions are purely governed by kinematics of deformation;
- determination of the equivalent stress and strain from boundary data (forces, displacements) and development of valid approximate relationships to be used in testing.

For the sake of brevity, we will report here selected numerical results, while a full account of the numerical study will be reported in a subsequent paper.

The SCS was discretized for three-dimensional static finite element analysis, using 8 node isoparametric brick type elements. The model comprised about 800 elements and was analyzed using the ABAQUS finite element program.[7] Uniform vertical displacements (d) were applied to the upper boundary of the specimen, while the motion of the lower boundary was constrained in the vertical direction only. The analysis allowed for large deformations (geometrical nonlinearities) and large strains. The material constitutive response was modeled by a bilinear representation (elastic and isotropic hardening plastic). Two generic materials were modeled, with different tangent plastic moduli (Table 1) but with the same elastic (Young) modulus, Poisson's ratio and yield stress. These materials, were selected to represent a typically "soft" and a "hard" material, to cover two extreme types of material response. We have made here no attempt to investigate different constitutive models.

Numerical Results

Boundary conditions for the gage section

The first point to be addressed is that of the boundary conditions which are imposed to the gage. In other words, for a given global displacement, what is the influence of the stiffness of the cylindrical sections of the SCS. A verification of the vertical displacement of two symmetrically located edge points on the gage section showed that the two points experience identical vertical displacements, regardless of the kind of material. Fig. 3 shows the relationship between the prescribed vertical displacement, d, and the local vertical displacement experienced by the gage (one of the two above-mentioned points), for the two kinds of materials.

TABLE 1—CONSTITUTIVE PARAMETERS FOR THE TWO KINDS OF MODEL METELS USED IN THE NUMERICAL SIMULATIONS OF THE SHEAR COMPRESSION SPECIMEN (SCS)

Material	Yield Stress (MPa)	Poisson's Ratio	Young's Modulus, E (GPa)	Hardening Modulus
"Hard"	400	0.33	210	E/100
"Soft"	400	0.33	210	E/500

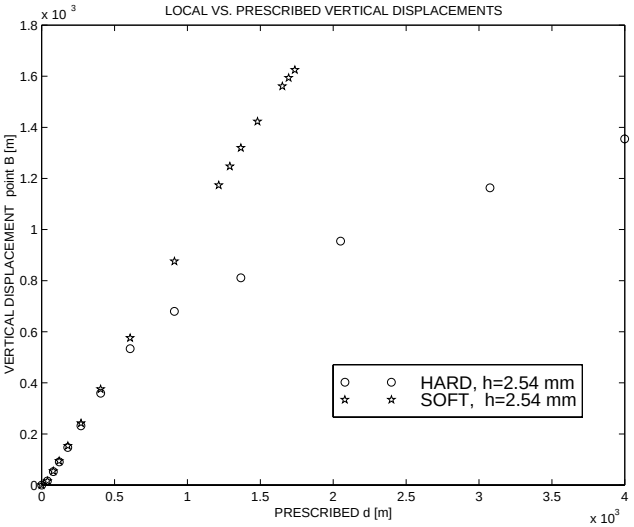

Fig. 3—Computed displacements of a representative point on the gage section, as a function of the prescribed vertical displacement. Note that for the "soft" material, there is a one to one correlation between these two factors, indicating that the cylindrical sections of the SCS do not alter the specimen stiffness.

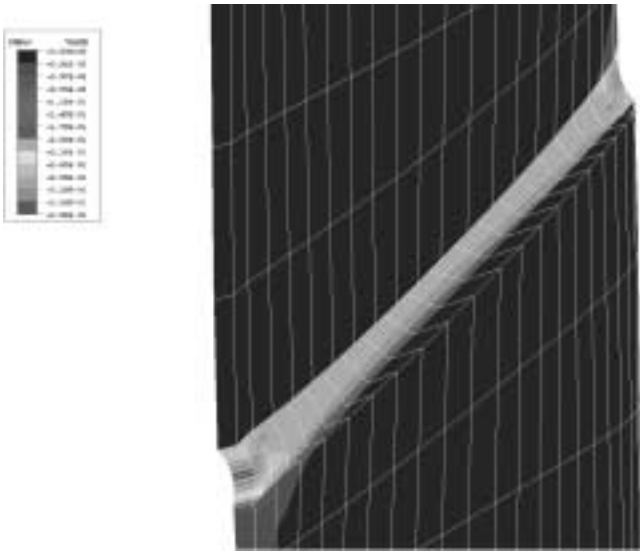

Fig. 4—Computed equivalent plastic strain, in the local gage section coordinate system. Note the uniformity of the deformation in the gage section. Most of the gage experiences strain levels in the range of 0.298–0.328 in this case.

For the "hard" material, the local displacement is identical to the prescribed displacement for only a limited range (up to $d = 0.7$ mm). By contrast, the local and prescribed displacements are virtually identical for the "soft" material for the overall prescribed displacement range. Similar additional results were obtained when the gage height, (h), was reduced to half its current value (Fig. 1), all other parameters being kept unchanged. The relation between local and prescribed displacements remains as before, with the distinction that the matching range for the "hard" specimen is now reduced to about half its previous value, i.e. about 0.35 mm.

At this stage, it is concluded that the boundary displacements are identical to those experienced by the gage section for a "soft" material, regardless of the gage height. For the "hard" material, there is a limited range of one to one correlation between these two displacements, which is also scaled by the gage's height.

Stress and strain fields

The calculated stress and strain components are referred to the current (deformed) configuration, i.e., true stress and strain. The shear strain and shear stress distributions were found to be rather uniform in the gage of the SCS, regardless of the material. Typical equivalent plastic strain and (Mises) stress fields are plotted as contours in Figs. 4 and 5, respectively. These figures confirm the relative uniformity of the equivalent stress and strain fields in the gage section.

Next, an element located at the center of the gage section was "monitored", being considered as representative of the field quantities in the gage section, on the basis of the

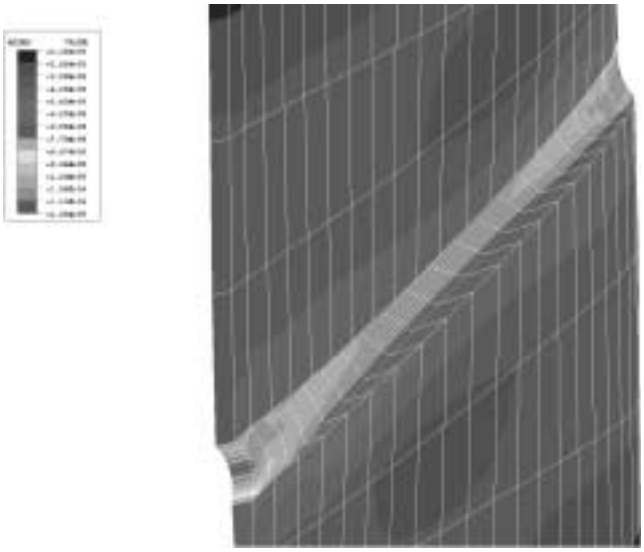

Fig. 5—Calculated (Mises) equivalent stress for the strain levels of Fig. 4, in the local gage coordinate system. Note the uniformity of the stress in the section gage. Most of the gage experiences stress levels in the range of 924–1000 MPa in this case.

uniformity of the stress and strain components. While additional detailed results will be reported elsewhere, the stress and strain field are clearly three-dimensional, of a nature which is not amenable to a simple analytical description such as simple shear. Examination of the strain components indicates, as expected, a dominance of the ε_{12} shear strain component. For the representative element, the equivalent stress–plastic strain relationships for the "hard" and the "soft" materials have been plotted in Fig. 6. It can be noted that the equivalent stress–plastic strain relationship is virtually identical to the prescribed constitutive behavior (Table 1). This observation was found to be independent of the gage height. While such a result is not only expected, it nevertheless adds to the validation of the specimen through numerical analysis.

Therefore it can be stated that the stress and strain fields are reasonably uniform in the gage section. The stress and strain state is more complex than that corresponding to simple shear. However, the calculated equivalent stress–plastic strain relationship accurately reproduces the prescribed constitutive law.

Simple Relationships for Stress and Strain

The next step is the identification of a simple relationship expressing the nominal equivalent stress (σ_{eq}), plastic strain (ε_{eq}) and strain rate ($\dot{\varepsilon}_{eq}$) in the specimen in terms of the geometrical parameters of the SCS and the boundary displacement and load. The following relations, based on the numerical results, are proposed:

$$\varepsilon_{eq} = \frac{d}{h}\ ;\ \dot{\varepsilon}_{eq} = \frac{\dot{d}}{h} \tag{1}$$

$$\sigma_{eq} = 0.85(1 - 0.2\varepsilon_{eq})\frac{P}{\phi t}. \tag{2}$$

As shown in Figs. 7 and 8, these simple approximations hold very well, irrespective of the gage height, for equivalent strains of typically $\varepsilon_{eq} = 0.4$ for the "hard" material and $\varepsilon_{eq} = 1$ for the "soft" material. Beyond this strain level, the simple relationships increasingly underestimate the stress and overestimate the strain, as the deformations get larger. As an example, for the soft material and larger gage height of Fig. 8, the last approximated point ($\varepsilon = 1.23, \sigma = 715$ MPa) underestimates the stress by about 12%, while it overestimates the strain by about 20%, with respect to the calculated point ($\varepsilon = 1.02, \sigma = 812$ MPa). More accurate relationships than Eqs (1) and (2) could of course be devised, but this would impair the simplicity of the approximation, which is what makes it attractive. It also appears that additional numerical modeling is required before the simple relationships can be extended to higher strains.

Consequently, geometrical parameters and measured loads and displacements can be used to determine in a straightforward and simple manner the equivalent true stress–true strain relationship.

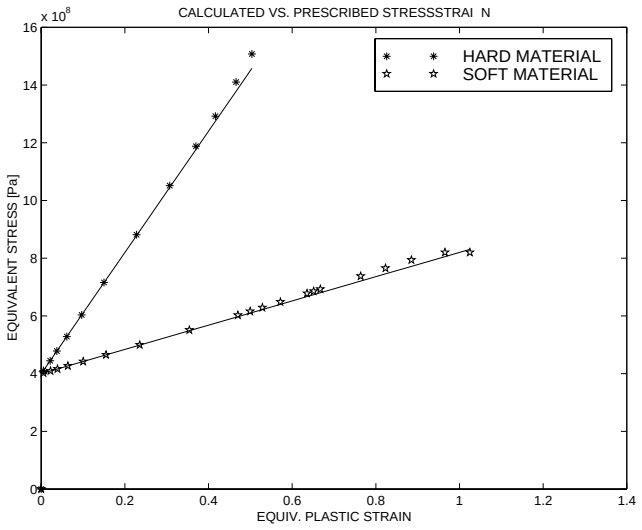

Fig. 6—Equivalent stress–equivalent plastic strain calculated in the element located at the center of the gage section, at mid-thickness. The solid line indicates the prescribed constitutive behavior of the material. Note that the prescribed constitutive behavior of both types of materials (see Table 1) is faithfully recovered by the calculation for the two materials.

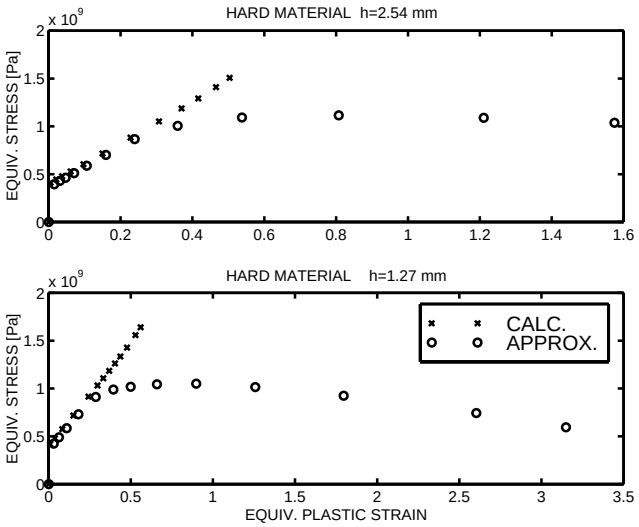

Fig. 7—Computed and approximated (Eqs (1) and (2)) equivalent stresses and plastic strains for the "hard" material with two gage heights.

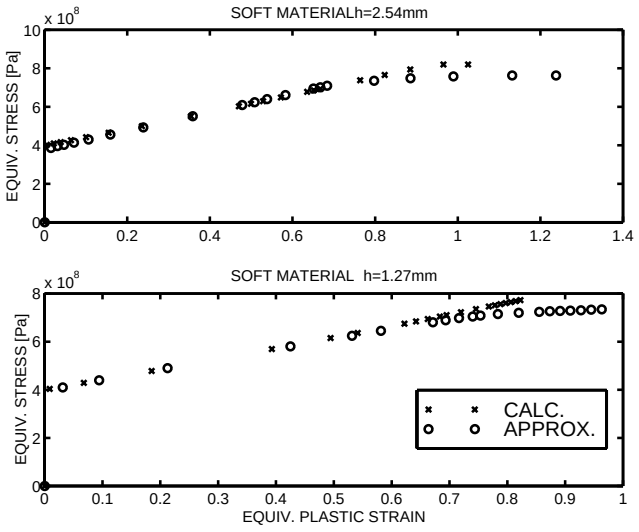

Fig. 8—Computed and approximated (Eqs (1) and (2)) equivalent stresses and plastic strains for the "soft" material with two gage heights.

At this stage, the results presented in this section will be used to process experimental data as reported in the next section.

Experimental Results

Material and Specimens

The goal of the experiments reported in this section is to validate the approach embedded in the use of the SCS for constitutive behavior testing. Therefore, the experiments consist of comparing the stress–strain relationships obtained in simple compression of cylinders (CS) to those obtained by using the SCS through the use of Eqs (1) and (2). The material selected was OFHC (copper), obtained in the form of a 12.54 mm diameter bar. The material was tested in the as received form without any thermal treatment, e.g., annealing. Additional testing was carried out on other materials (annealed Ti6Al4V and 6061-T6 aluminum alloy), but for the sake of brevity, the present paper will only discuss the results obtained for OFHC. The SCS specimens were machined with two gage heights (nominally 2.54 mm and 1.27 mm) and the compression cylinders were 7.5 mm in diameter and varying length to modify the strain rate.

Testing was first carried out in a screw driven INSTRON machine (displacement control) to "calibrate" the SCS versus the cylindrical specimens. High strain rate compressive testing was carried out on a Kolsky (split Hopkinson) pressure bar.[8]

Static Testing

Two cylinders (7.5 mm long) each were compressed at nominal strain rates of 10^{-4} s^{-1}. Two SCS were also tested at a strain rate of 10^{-3} s^{-1}. Testing was carried out by compressing the cylinders and SCS between lubricated (petroleum jelly) steel platens. A typical stress–strain relation determined using the cylinders and the SCS is shown in Fig. 9. While the curves are very similar, the stresses obtained from the cylindrical specimen are elevated by a constant stress level of about 50 MPa, with respect to the SCS data. Such a shift was repeatedly observed and a possible cause may be frictional effects between the specimen and the platens, despite careful lubrication. Indeed, some degree of barreling was observed to develop during the test. Frictional effects are expected in both types of compressive tests. However, their effect is obviously smaller for the SCS specimen, for which the gage deformation is not altered by friction, nor is it subject to barreling as opposed to the cylinder.

To illustrate the effect of friction on the stress only, assume the stress state in the cylinder can be described by the following stress tensor:

$$\boldsymbol{\sigma} = \begin{bmatrix} \sigma & \tau & \tau \\ \tau & 0 & 0 \\ \tau & 0 & 0 \end{bmatrix}, \tag{3}$$

where σ and τ represent normal and shear components. Let μ, Coulomb coefficient of friction, relate the normal and shear stress, $\tau = \mu\sigma$ (beyond impending slip, for the sake of simplicity). The equivalent stress (σ_{eq}) can now be written from the inner multiplication of the deviatoric stress tensor **s** so that:

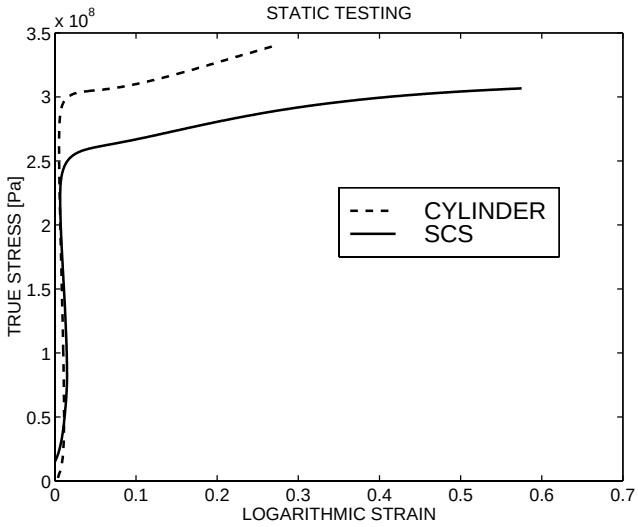

Fig. 9—Experimental results showing the comparison of the quasi-static stress–strain (strain rate, 10^{-4} s^{-1}) curve of OFHC copper, obtained using compressed cylinders and SCS. The 25 MPa offset of the cylindrical specimen is most likely the result of interfacial friction with the loading platens.

$$\frac{3}{2} s_{ij} s_{ij} = \left[6\mu^2 + 1\right]\sigma^2 = \sigma_{eq}^2. \tag{4}$$

When $\mu = 0$ (frictionless), the equivalent stress is equal to the uniaxial stress, but for any other values of μ, the equivalent stress will be higher than the uniaxial, as observed here. From Eq (4), a calculated value of $\mu = 0.27$ is sufficient to cause the observed 20% elevation of stress. It should also be noted that the investigated material is close, in a sense, to the "soft" material that was selected for the numerical simulations. A detailed analysis of frictional effects can be carried out for the SCS in order to optimize its geometry, as was done for the SHPB standard specimens. Moreover, it should be noted that barreling of the gage section of the SCS was quite seldom observed in our experiments, and this was only the case for relatively large strains.

It can thus be concluded that the SCS yields stress–strain values which are quite comparable to those obtained from uniaxial tests, without inherent restrictions of necking, barreling or friction.

Dynamic Testing

Dynamic testing was carried out on a Kolsky (split Hopkinson) pressure bar. For the sake of brevity, we will not describe the technique, and the reader is referred to Kolsky[8] for further details. However, the following specific points must be noted. With this technique, the boundary conditions applied to the deforming cylinder, namely two interfacial—incident and transmitted—forces (F) and displacements (u) are determined as a function of time, using the strain gage signals on the bars. Let the subscripts i, r, and t denote incident, reflected and transmitted signals, respectively. E denotes the Young's modulus of the bars, A their cross sectional area (identical here to that of the SCS), and c is the longitudinal bar wave velocity, ($\sqrt{E/\rho}$ where ρ is the bar material density). The forces and displacements at the interface between the bar and the specimen are given by:

$$\begin{cases} P_i(t) = EA\,[\varepsilon_i(t) + \varepsilon_r(t)]\ ;\ P_t(t) = EA\varepsilon_t(t) \\ u_i(t) = c\displaystyle\int_0^t [\varepsilon_i(t) - \varepsilon_r(t)]\,dt\ ;\ u_t(t) = c\int_0^t \varepsilon_t(t)dt. \end{cases} \quad (5)$$

Consequently, the applied displacement d and load P (Eqs (1) and (2)) are given by

$$d(t) = u_i(t) - u_t(t)\ \ ;\ \ P(t) = \frac{P_i(t) + P_t(t)}{2}. \quad (6)$$

It must also be noted that in these formulas, force equilibrium is not assumed to hold, *a priori*, as is commonly done in compressive testing of materials in a Kolsky (split Hopkinson) pressure bar. Equations (5) and (6) will be referred to as "complete" without resorting to the assumption of force equilibrium. Once equilibrium is established "simplified" relations, in which $P_i(t) = Pt(t)$, can be derived from Eq (5), that is when

$$\varepsilon_i(t) + \varepsilon_r(t) = \varepsilon_t(t). \quad (7)$$

At this stage, it is worth noting that whereas the global specimen equilibrium may require several microseconds to establish, the local gage section equilibrium is reached in a much shorter duration due to the small gage dimensions, thus implying a uniform deformation state in the gage. It is the latter which is relevant to the SCS. However, stress–strain calculations using complete and simplified relations will yield different results for initial strain whose extent is dictated by the strain rate. Past this initial strain, both formulations yield the same result. Such a limitation is a characteristic of the Kolsky bar testing, regardless of the specimen geometry.

Consequently, we adopted the following approach: for each test, the stress–strain relationship was calculated using both the complete and the simplified formulas, and the average stresses and strains were then calculated using Eqs (1) and (2), as mentioned.

A Comparison between SCS and Cylinders

The range of dynamic strain rates from 2500 s^{-1} to 18000 s^{-1} was investigated using cylindrical compression specimens (CS) and SCS specimens. The range of strain rates from 2500 s^{-1} to 10000 s^{-1} was characterized with cylindrical specimens. The range of strain rates from 7000 s^{-1} to 18000 s^{-1} was characterized with SCS. Selected comparative results are shown for typical strain rates which are achievable by both techniques. In Fig. 10, we have plotted comparative typical results obtained at strain rates of 7000 and 9000 s^{-1}. This figure shows the high level of similarity between the results obtained with the two distinct techniques, beyond an initial strain of about 0.15.

Finally, the flow stress at a strain of 0.2, as a function of the strain rate, is shown in Fig. 11. Data obtained using both cylindrical and SCS specimens have been plotted on the same figure. Additional data points have been inserted, based on the results of Nemat-Nasser *et al.*[9] The current results from the SCS specimen capture the trend and magnitude of the flow stress in the range of strain rates investigated. The characteristic rate sensitivity of OFHC copper is noticeable.

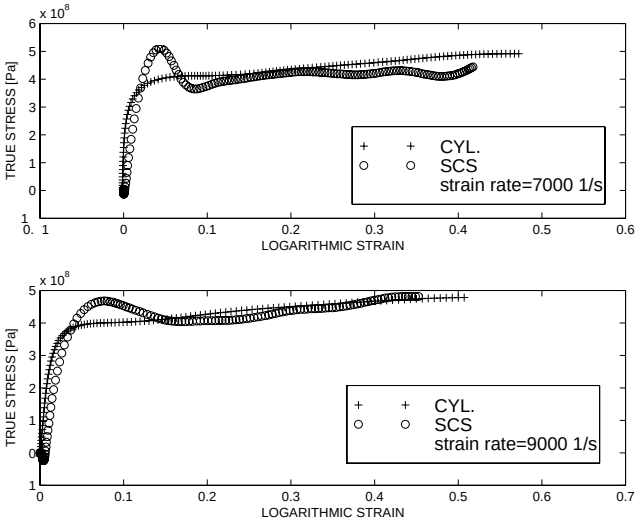

Fig. 10—Experimental results showing the comparison of the dynamic stress–strain curve of OFHC copper, obtained using compressed cylinders and SCS at strain rates of 7000 s^{-1} and 9000 s^{-1} respectively.

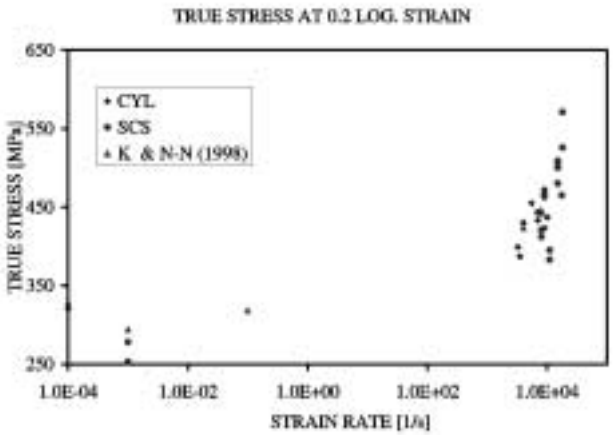

Fig. 11—Strain rate dependence of the flow stress of OFHC copper at an equivalent plastic strain of 0.2. The strain rate range varies from 10^{-4} to 18 $\times$ 10^3 s^{-1}. The results have been obtained using compression cylinders and SCS. Results by Nemat-Nasser *et al.*[9] have been added for comparison purposes.

This figure illustrates the potential of the new SCS to yield data at higher strain rate, i.e 10^4 s^{-1} and above, where little data is available.

Discussion

A new specimen geometry has been proposed for large strain constitutive testing of materials. The specimen has been extensively analyzed to provide a clear description of the stress and strain state in the gage section. The analysis shows that the deformation of the gage section is far from being the ideal case of pure shear, or more realistically simple shear. However, such assumptions are not needed here, as it is shown that the SCS deformation is driven by the prescribed

displacements, and more important, that a simple relation can be established and validated between boundary loads and displacements on the one hand, and equivalent true stress and true plastic strain on the other hand. This relation is valid for equivalent plastic strain values of up to 1. Additional numerical modeling is required to extend these simple relations to larger strains. For the less ductile materials (e.g. the "hard" material), these relations apply to a narrower strain rage.

The predominant deformation mode of the SCS is shear. Large deformations can be thus be achieved for ductile materials without the usual plastic instabilities or barreling, which are inherent to uniaxial testing of materials. Validation of the specimen geometry has been performed experimentally, by comparing results from cylindrical specimens and SCS. The high degree of similarity between the two is expected, but remains a necessary condition to the use of this specimen. The geometry of the specimen lends itself to simple insertion in a dynamic compressive apparatus such as the Kolsky (split Hopkinson) bar. With this technique, the constitutive behavior can be obtained easily using standard signal processing procedures for the Kolsky (split Hopkinson) pressure bar. The range of attainable strain rates is dictated by the gage height h. With the present configuration, the covered range was 7000 s^{-1} to 18000 s^{-1}. Such a range overlaps partly with that attainable with conventional cylindrical specimens, but is nevertheless extends beyond the upper limit of the Kolsky pressure bar, 10^4 s^{-1}. Smaller gage heights can easily be realized to reach higher rates. In a series of recent experiments, to be reported in the future, strain rates of 4.7×10^4 s^{-1} were reached. As such, the important gap between conventional Kolsky/SHPB experiments and plate impact[6] can be partially filled. Moreover, the SCS is not restricted to investigations of high-strain-rate behavior. By suitably choosing the gage dimensions, one can expect to attain strain rates in the range of 1 s^{-1} to 100 s^{-1} using conventional material testing frames. This range of strain rates is a traditional "twilight zone" in constitutive testing where relatively little data is available due to lack of reliable testing techniques. Finally, additional applications of the SCS, such as shear localization or dynamic recrystallization studies, can be thought of, which take advantage of the dominant state of shear deformation in the specimen.

Conclusions

- A new specimen geometry, the shear compression specimen (SCS), has been developed for large strain testing of materials. The dominant deformation mode in the gage section is shear.

- The specimen has been analyzed numerically to identify the stress and strain state in the gage. The stresses and the strains were both found to be uniform in the test gage section. For a typical gage element, the stress–strain relationship follows closely the prescribed constitutive law, irrespective of the material parameters, or the gage geometry.

- Simple relations were developed and assessed to relate the equivalent stress and equivalent plastic strain to the applied loads and displacements. Both the equivalent strain and the strain rate are inversely proportional to the gage height.

- The specimen was further validated through actual experiments carried out on OFHC copper, by comparing results obtained with the SCS to those obtained with compression cylinders. The SCS enables seamless investigations over a large range of strain rates, from the quasi-static regime, through intermediate strain rates (1–100 s^{-1}), up to very high strain rates (2×10^4 s^{-1} in the present case).

- The SCS is particularly attractive as it is easy to use in standard compression apparatus both in the static and dynamic regimes, while the stress–strain relationships are kept simple.

References

1. Campbell, J.D. and Ferguson, W.G., "The temperature and strain rate dependence of the shear strength of mild steel," Phil. Mag., **21**, *63–75 (1970).*

2. Duffy, J., Campbell, J.D., and Hawley, R.H., "On the use of a torsional split Hopkinson bar to study rate effects in 1100 O aluminum," J. Appl. Mech., **38**, *83–91 (1971).*

3. Hundy, B.B. and Green, A.P., "A determination of plastic stress–strain relations," J. Mech. Phys. Solids, **8**, *16–21 (1954).*

4. Meyer, L.W. and Manwaring, S., in Metallurgical Applications of Shock Wave and High-Strain Rate Phenomena, Murr, L.E. et al. *Eds, Marcel Dekker Inc. NY (1986).*

5. Klepaczko, J.R., "An experimental technique for shear testing at high and very high strain rates," Int. J. Impact Eng., **46**, *25–39 (1994).*

6. Clifton, R.J. and Klopp, R.W., in Metals Handbook: Mechanical Testing, **8**, *ASTM, Metals Park, Ohio (1986).*

7. Hibbitt, Karlsson and Sorensen, Inc. ABAQUS/Standard User's Manual, Version 5.6. (1996).

8. Kolsky, H., "An investigation of the mechanical properties of materials at very high rates of loading," Proc. Phys. Soc. London, **62-B**, *676–700 (1949).*

9. Nemat-Nasser, S., Ni, L., and Okinaka, T., "A constitutive model for fcc crystals with application to polycrystalline OFHC copper," Mech. of Materials, **30**, *325–341 (1998).*